ELSEVIER

Contents lists available at ScienceDirect

Journal of Cleaner Production

journal homepage: www.elsevier.com/locate/jclepro





Life cycle assessment of inkjet printed perovskite solar cells

Tobechi Okoroafor ^a, Amani Maalouf ^a, Senol Oez ^b, Vivek Babu ^b, Barbara Wilk ^{c,d}, Shahaboddin Resalati ^{a,*}

- ^a Oxford Brookes University, Headington Campus, Gipsy Lane, Oxford, OX30BP, UK
- ^b Saule Technologies, Wrocław Technology Park, 11 Dunska, Wrocław, 54-427, Poland
- ^c Saule Research Institute, Wrocław, 54-130, Poland
- d Department of Semiconductor Materials Engineering, Wroclaw University of Science and Technology, Wroclaw, 50-370, Poland

ARTICLE INFO

Handling Editor: Zhifu Mi

Keywords: Perovskite solar cell Life cycle assessment Inkjet printing Green solvents Spin coating

ABSTRACT

Perovskite solar cells (PSCs) have moved to the forefront of emerging thin-film solar cell research in just a decade, demonstrating the most promising efficiency records. These technological advancements however, were primarily tested at laboratory scale and there remains significant issues in relation to the scalability of the deposition methods utilised. Inkjet printing, initially used for printed electronics, has recently been applied to solar cell production and demonstrated promising potential for scaling up. Despite various studies that have assessed the technical feasibility of utilising inkjet printing, their environmental performance has not been investigated. This paper, for the first time, presents a comprehensive Life Cycle Assessment (LCA) study of inkjet printing-based PSCs, on a cradle-to-gate basis using GaBi LCA software. The results were compared with those of spin-coating, as the most widely studied deposition method, and demonstrated significant improvement in all impact categories. Global warming potential (GWP) and cumulative energy demand (CED) were used as proxies to compare results obtained in this paper with available studies in the literature. The comparison demonstrated that inkjet printing of PSCs had a GWP and CED of 7.54 kg CO₂eq/m² and 200.18 MJ/m² while spin-coating had a reported median value of $74.5~kg~CO_2eq/m^2$ and $1204~MJ/m^2$ respectively. This suggests considerable environmental advantage for the inkjet method. The paper also assesses a novel green solvent-based precursor ink investigating the environmental benefits of eliminating the toxic and hazardous solvent materials commonly used in wet chemical deposition of perovskite layers. The green solvent-based precursor ink results demonstrated significant improvement over conventional solutions with up to six orders of magnitude lower impacts. The LCA results obtained in this paper contributes to forming a full assessment of the development of scalable deposition methods such as inkjet printing by highlighting their environmental hotspots and advantages. The paper also identifies potential opportunities for perovskite precursor ink material composition improvements for sustainable development of PSCs. This will assist in addressing their associated environmental concerns in relation to the use of high impact toxic solvents.

1. Introduction

Perovskite solar cells (PSCs) have captured the attention of the research community ever since its invention in 2009. In just a decade, the efficiency of the technology has increased from around 3%–25.5% (Roy et al., 2020). Such performance boosts took conventional silicon solar cells more than 40 years to achieve as indicated by the NREL best research solar cell efficiency chart (NREL, 2022). Perovskites represent a family of crystalline compounds that adopt a similar crystal structure as the parent mineral calcium titanate CaTiO₃. The structure was

discovered in 1839 by Gustav Rose and named after Russian mineralogist Count Aleksevich von Petrovski (Tilley, 2016). This class of materials can be generally described by the ABX₃ formula, where the A- and B-sites are occupied by positively charged cations and the X-sites are occupied by negatively charged anions to achieve charge neutrality (Jung et al., 2020). Much more complex compositions can be obtained by intermixing of suitable cation- or anion combinations at the A-site (A_{1-x}A'_xBX₃), B-site (AB_{1-x}B'_xX₃), X-site (ABX_{3-x}X'_x) or even at all three possible sites at once (A_{1-x}A'_xB_{1-y}B'_yX_{3-z}X'_z) (Ünlü et al., 2021). In the perovskite structure, the large A-site cations occupy the corners of the

E-mail address: sresalati@brookes.ac.uk (S. Resalati).

 $^{^{\}ast}$ Corresponding author.

unit cell, while the smaller sized B-site cations occupy the center of the unit cell. The X-site anions are centered at the faces of the unit cell, forming an octahedral coordination polyhedron around the central B-site cation. The A-site cation is coordinated to 12 X-site anions that form a cuboctahedral array around the A-site cation. The most common perovskite used to manufacture solar cells are CH3NH3PbI3 and CH (NH₂)₂PbI₃ alongside mixed halide and complex mixed A-site compositions (Ünlü et al., 2020). PSCs are usually assembled in either the mesoscopic or planar device architecture with the difference being the absence of a mesoporous layer in the latter (Zhao and Zhu, 2016). The solar cells with n-i-p configuration, usually have a transparent conductive contact (e.g. fluorine-doped tin oxide), a compact metal oxide electron transport layer (e.g. SnO2, TiO2), a perovskite absorber layer (thickness 150-1000 nm), and a hole transport layer (e.g. Spiro-MeOTAD, PTAA). The process is finished with a thermally evaporated metal back contact (gold or silver) (Celik et al., 2016). PSCs using flexible substrates such as Polyethylene terephthalate have the potential to be manufactured in different shapes, enabling the cells to be applied to wearable and portable devices alongside incorporation in buildings and other architectural designs (Liang et al., 2021). Also, due to PSCs exceptional radiation resistance, it is seen as the next generation space solar cell technology (Tu et al., 2021).

The efficiency of PSCs is strongly influenced by the formation of the perovskite absorber layers (Roy et al., 2020). Researchers have established different methods through which the perovskite precursor ink can be deposited affecting the absorber layer properties such as crystallinity and uniformity. Those factors have a direct impact on the resulting layer quality and subsequently on the performance of the perovskite solar cell. The most common methods of depositing the perovskite precursor ink on lab scale are spin coating and thermal evaporation (Roy et al., 2020). However, techniques such as inkjet printing, drop casting, doctor blade coating, slot die coating, and spray coating were explored to overcome the limitations associated with large scale deployment of PSCs by spin coating method (Roy et al., 2020). Previous studies showed that PSCs performed better than existing solar cell technologies in terms of key performance indicators (such as high energy conversion efficiency, low material usage, overall cost, and production process). Although the challenges pertaining to the scalability of the deposition methods utilised still exist (Ansari et al., 2018). In this context, the usage of expensive materials such as gold and silver, as well as energy-intensive techniques such as vapour deposition and spin coating need to be carefully considered for better environmental profile and scalability potential. Stability of the deposited perovskite layer is also a problem encountered during fabrication of PSCs. Defects tend to occur in the bulk and at interfaces in the perovskite where photogenerated electrons and holes form resulting in a loss of active charge carriers (Wang and Jiang, 2021). Decomposition of the perovskite can subsequently happen due to these defects as they are sensitive to oxygen, heat, moisture, and ultraviolet light (Liu et al., 2020). Alteration of the perovskite using polymers, salts, and molecules have been proposed to reduce defect formation but they have different structures and tend to be immiscible (Zhang et al., 2021). Modifiers that have physicochemical conformity with the perovskite are thus preferred (Zhang et al., 2021). One of such modifiers proposed by researchers is to use CsPbBr3 nanocrystals to modify the interfaces of the perovskite active layer. This would effectively reduce defects developing at the interfaces between the perovskite layer and other adjacent layers such as the hole transporting layer, increasing interface electron transportation (Zhang et al., 2021).

Inkjet printing has been broadly applied to printed electronics as a non-contact deposition method, allowing for the perovskite precursor ink to be applied on a wide variety of materials and shapes (Roy et al., 2020). This is ideal for PSCs with flexible substrates (Zhang et al., 2020). The technology offers promising potential for large industrial scale-up. The technique has the advantage of being low cost, scalable, and flexible (Wei et al., 2014). This technique has also been used by researchers obtaining stable performances for their PSC using the precursor solution

based on a non-hazardous solvent system (Wilk et al., 2021). The utilisation of non-toxic solvent solutions offers significant large scale industrial development benefits. This due to the conventional precursor solutions, widely applied to processing perovskite layers, being typically based on highly toxic solvents (Wilk et al., 2021). Most of the solvent systems described in literature are hazardous to human health and ecologically worth considering adequate alternatives. The aprotic polar organic solvents widely used for fabrication of perovskite solar cells with high power conversion efficiencies include the toxic compounds N, N-dimethylformamide (DMF) and its derivative N, N-dimethylacetamide (DMAC), skin permeating dimethyl sulfoxide (DMSO), and carcinogenic N-methyl-2-pyrrolidone (NMP). Investigating less hazardous or ideally non-toxic alternative solvent systems are desirable for the safe processing of organic-inorganic hybrid perovskites in the lab and for their safe applicability in industrial environment.

The environmental performance of solar cells has been investigated in detail in the past decade to inform the development of emerging solar cells and the associated impact of the materials and processes utilised. Life Cycle Assessment (LCA) is a well-established standardised assessment method that aids investigation of the environmental impacts of a product or service. The system boundary can include all impacts from raw material extraction through use and then disposal or recycle (Maranghi et al., 2019). Table 1 shows the ranges and median global warming potential (GWP) and cumulative energy demand (CED) obtained from LCA studies conducted on first, second and third generation solar cells. PSCs are seen to be competitive environmentally with the other technologies especially when compared with conventional silicon based solar cells. Due to the ongoing research on PSCs, LCA studies conducted on the solar cell have a wider range than more established technologies. This is due to the different material configurations and deposition methods used in the studies.

Table 2 demonstrates the numerous individual LCA studies that have investigated the environmental performance of PSCs using various deposition methods, with the majority of them studying spin coating. Spin coating of the perovskite absorber layer cannot be deployed commercially due to its limitations mentioned earlier. It has become paramount that detailed environmental assessments need to be conducted on other deposition methods such as inkjet printing with a promising scale-up potential, in parallel to the technical endeavours, to support the decision making process.

This paper, for the first time, evaluates the environmental impact of producing PSCs using inkjet printing. It builds up on the previous work on the green solvent precursor solution developed by Wilk et al. (2021) to provide a true environmental performance aligned with the industry needs and requirements. This paper focused on assessing the environmental health and energy impacts from materials and manufacturing stages including the deposition methods and precursor inks. The analyses contribute to the extensive work being undertaken in the emerging thin-film solar cell technologies by identifying the environmental

Table 1Summary of GWP and CED results of LCA studies on thin film and silicon based solar cells (Adapted from vidal et al., (Vidal et al., 2021b)).

Solar Cell	PCE (%)	Range (GWP [kg CO ₂ eq/ m ²])	Median (GWP [kg CO ₂ eq/ m ²])	Range (CED [MJ/m ²])	Median (CED [MJ/ m ²])
PSC	12.55	1952–27	90.2	19,712–298	1489.4
Mono-Si	14.8	404-146	167.7	4395-3577	3986.4
Multi-Si	14.1	290-94	156.4	3398-1933	2367.4
a-Si	7	82-58	69.9	1057-1050	1053.5
CdTe	11.9	62-43	52.1	752-745	748.5
CIGS	11.7	89-26	61.2	1219-1205	1211.0
CZTS (Resalati et al., 2022)	11	82.2	82.2	2225.5	2225.5

 Table 2

 Existing LCA studies on single junction and tandem PSCs.

Reference	Deposition	Efficiency (%)	Life cycle stages	Location
Single junction PSCs				
This study	Inkjet Printing	11.4	Cradle to gate	Europe
(Alberola-Borràs	Spin-coating/	10.4-15	Cradle to	Europe
et al., 2018a)	Screen printing		gate	•
Celik et al. (2016)	Spray/vacuum	15	Cradle to	USA
	deposition		gate	
Espinosa et al. (2015)	Thermal co- evaporation/Spin coating	11.4–15.4	Cradle to gate	Southern Europe
Gong et al. (2015)	Spin-coating + dipping/spin coating/thermal co- evaporation/spray coating	9.1–15	Cradle to grave	USA
Itten and Stucki (2017)	Spin-coating + dipping/Thermal evaporation and slot die/Thermal evaporation of Pbl2 and slot die coating of MAI	13.8–18.3	Cradle to grave	Europe
Ibn-Mohammed et al. (2017)	Spin-coating/ vapour deposition	15.1–21.1	Cradle to grave	United Kingdom
Zhang et al. (2015)	Spin coating/Spin- coating + dipping	6.5	Cradle to	USA
Sánchez et al. (2019)	Spin-coating, FIRA	17.3	Cradle to	Europe
Sarialtin et al. (2020)	Spin-coating	11.5–14.5	Cradle to	Europe
Serrano-Lujan et al. (2015)	Spin-coating/ Vapour deposition/ Thermal co- evaporation	6.4–15.4	Cradle to gate, Cradle to grave	Europe
Tandem PSCs	1			_
Itten and Stucki (2017)	Thermal evaporation & slot die	23.8	Cradle to grave	Europe
(Monteiro Lunardi et al., 2017)	Spin-coating	27	Cradle to grave	Europe
Celik et al. (2016)	Spin-coating	6–24	Cradle to gate	USA

hotspots of materials and processes related to perovskite solar cells. The results will assist technology developers and LCA practitioners in addressing the limitations of existing studies in the field.

2. Life cycle assessment methodology

Environmental and human health consequences were assessed in this study using an LCA approach according to ISO 14040 (International Organization for Standardization, 2006a) and ISO 14044 international standards (International Organization for Standardization, 2006b). Calculations were performed using the GaBi LCA software (GaBi ts V9.2), which is extensively used for environmental and economical sustainability modelling and assessment (GaBi, 2022) showing adequate competency (Speck et al., 2016). LCA studies have four distinct stages including 1) Goal and Scope definition, where key steps including system boundaries are defined, 2) Life Cycle Inventory Assessment, where all the inputs and outputs from the system are tracked, 3) Impact Assessment, where the inventory data is translated into environmental and health indicators, and 4) Interpretation, where appropriate sensitivity and uncertainty analyses are applied to the results and the analysis is translated into meaningful messages for the end users.

2.1. Goal and Scope

The goal of this study is to evaluate the environmental performance of PSCs manufactured using green solvent-based perovskite precursor inks. As perovskite cells are currently not being manufactured on an industrial scale, the LCA study here was conducted using lab-based cells. When large scale production processes for PSCs become available, the LCA methodology applied here can adequately be used to evaluate plant environmental impact.

Previous studies have demonstrated that manufacturing processes and materials used for perovskite cell production constitute the majority of its environmental impact (Gong et al., 2015). Large-scale commercialisation of PSCs has yet to take place, hence, uncertainties exists in relation to their operation and end of life phases. The system boundary selected for this study, therefore, was based on a cradle-to-gate approach, limiting the scope to assessing the environmental impact of PSCs from raw material extraction till the factory gate. A cradle-to-gate approach is commonly applied by other existing LCA studies related to emerging solar cell technologies due to limited data on their in-use and end of life phases (see Table 2). Electricity generation is the function of PSCs, therefore, a functional unit based on 1 kWh electricity generation was used in this study. This was also taken as the reference flow.

PSCs with n-i-p configuration are usually made up of a fluorine-doped tin oxide (FTO) coated glass substrate, a $\rm TiO_2$ electron transport layer, perovskite absorber, Spiro-MeOTAD hole transport layer, and a gold back contact (Celik et al., 2016). Table 3 presents the device architecture of the modelled perovskite solar cell alongside other alternative materials that can be used for each layer. The modelled LCA in this paper is based on the work carried out by Wilk et al. (2021) who have developed the green solvent-based precursor ink adopted.

The efficiency of the modelled perovskite cell was 11.4% with the required area (6.45 cm²) to achieve the functional unit (1 kWh) calculated using the following equation (Amarakoon et al., 2018):

$$A = \frac{Lifetime\ Output\ (kWh)}{SI\ *\ PR\ *\ E\ *\ LT}$$

where.

 $A = Area (m^2)$

SI = Solar radiation (kWh/m²)

PR = Performance ratio (%)

E = Efficiency (%)

LT = Lifetime (yr)

The average solar radiation of the UK (850 kWh/m²) was selected for this study assuming an operational lifetime of 20 years in order to compare results with other solar cells. Alongside this a performance ratio of 80% was chosen as recommended by the International Energy Agency (Fthenakis et al., 2011). Given the comparative nature of the

Table 3Device Architecture of modelled PSCs and alternatives for each device layer.

Layer	Modelled Perovskite Cell (Wilk et al., 2021)	Alternative Chemical (Celik et al., 2016)
Front contact layer	PET/IZO	FTO, ITO
Hole transfer	PEDOT:PSS	Spiro-MeOTAD, P3HT,
layer		PTAA, CuSCN, CuI, NiO
Absorber	Cs _{0.1} [(HC	$CH_3NH_3PbI_xBr_{3-x}$
Layer	$(NH_2)_2)_{0.83}(CH_3NH_3)_{0.17}]_{0.9}Pb$	$CH_3NH_3PbI_xCl_{3-x}$
	$(I_{0.83}Br_{0.17})_3$	CH ₃ NH ₃ PbI ₃
Electron transport layer	C ₆₀	TiO ₂ , ZnO, Al ₂ O ₃ , SnO ₂
Back contact layer	Ag	Au, MoO _x /Al, C-Paste

analyses in this paper, the relative results are independent of the location of the study.

The process of manufacturing the modelled perovskite cell involves five steps. In the first step flexible indium zinc oxide (IZO) electrode grown on a polyethylene terephthalate (PET) substrate, using a roll to roll sputtering system, is etched in 15 wt% hydrochloric acid (HCL) and cleaned using isopropanol. This is followed by a further 2 min of cleaning using N₂ plasma (Wilk et al., 2021). The second and third steps involve a hole transport and absorber layer being deposited on the substrate. In order to manufacture the absorber, perovskite precursor ink is prepared by dissolving formamidinium iodide, methylammonium bromide, lead bromide, and lead iodide in γ -butyrolactone, 2-methylpyrazine, and dimethyl sulfoxide with thiosemicarbazine and formic acid used as additives to aid in the formation of stable Pb complexes (Wilk et al., 2021). The precursor ink and aforementioned additives are then printed using an inkjet printer. This is feasible as stability issues associated with inkjet printing of perovskite layer are improved by delaying the perovskite crystallisation and reinforcing the intermediate phase with the introduction of the additives thiosemicarbazine and formic acid. The solvent γ-butyrolactone even with the addition of 2-methylpyrazine and dimethyl sulfoxide does not have enough intermolecular binding energy to form stable perovskite layer as crystallisation is fast and unstable. Introducing the combination of thiosemicarbazine and formic acid as additives would result in forming a compact stable perovskite layer (Wilk et al., 2021). The hole transport layer was achieved by poly(3,4ethylenedioxythiophene):polystyrene sulfonate (PEDOT:PSS) dispersion which was modified using lead acetate additives to improve the characteristics of the interface. Electron transport thermal evaporation was used to deposit 30 nm of buckminsterfullerene (C₆₀). For the final step, a silver electrode was deposited using thermal evaporation (Wilk et al., 2021). Fig. 1 details the adopted system boundary in relation to the manufacturing steps explained above, from raw material extraction to the production gate.

2.2. Life cycle inventory analysis

Data used for the LCA in this study were primarily compiled from the data obtained from Wilk et al. (2021), and published literature. The database of GaBi LCA software was used to calculate the life cycle impact assessment of available materials (GaBi, 2022). The inventory data was complemented based on stoichiometric relationships and manufacturing processes reported in literature, when not available.

Inventory analysis is a key aspect of any LCA study as it quantifies all inputs and outputs alongside emissions of the studied materials or processes. Based on the system boundary (Fig. 1) a materials inventory table

has been constructed and presented in Table 4. It consists of the mass of materials and energy used per functional unit of the perovskite cell. The work of Gong et al. (2015) was adopted for the mass of HCL used in substrate cleaning, energy for spin coating deposition, thermal

Table 4Life Cycle Inventory of the assessed Perovskite cells producing 1 kWh of energy (Compiled by authors using aforementioned data sources).

	Input	Amount	Unit
Front Contact	Poly(ethylene terephthalate)	157.25	mg
	Indium	0.59	mg
	Zinc	0.02	mg
	Oxygen	0.51	mg
Cleaning	15 wt% HCL	44.83	mg
	Isopropanol	1290	mg
	Nitrogen for plasma	3.10	ml
	Energy for plasma	0.0037	MJ
Hole transport	PEDOT:PSS	0.26	ml
	Lead acetate	1.29	mg
	Energy for deposition (spin-coating)	0.012	MJ
	Energy for annealing	0.28	MJ
Absorber	Formamidinium iodide	5.29E-	mg
		07	
	Methylammonium bromide	7.10E-	mg
	•	08	Ü
	Lead bromide	2.51E-	mg
		07	Ü
	Lead iodide	1.74E-	mg
		06	Ü
	γ -butyrolactone	3.62E-	ml
	•	09	
	2-methylpyrazine	1.59E-	ml
	, 1, ,	09	
	Dimethyl sulfoxide	3.83E-	ml
	,	10	
	Cesium iodide	1.20E-	mg
		07	O
	Thiosemicarbazine	6.22E-	mg
		08	O
	Formic acid	6.97E-	ml
		11	
	Energy for ink preparation	0.0006	MJ
	Energy for deposition	0.0074	MJ
	Energy for post-treatment	0.0051	MJ
Electron	Buckminsterfullerene (C ₆₀)	0.00064	mg
transport	Energy for C ₆₀ and bathocuproine	0.0196	MJ
· · · · · ·	evaporation		-
Back contact	Bathocuproine	4.64E-	mg
	r ·	05	Ü
	Silver	7.68	mg
	Energy for silver evaporation	0.076	MJ

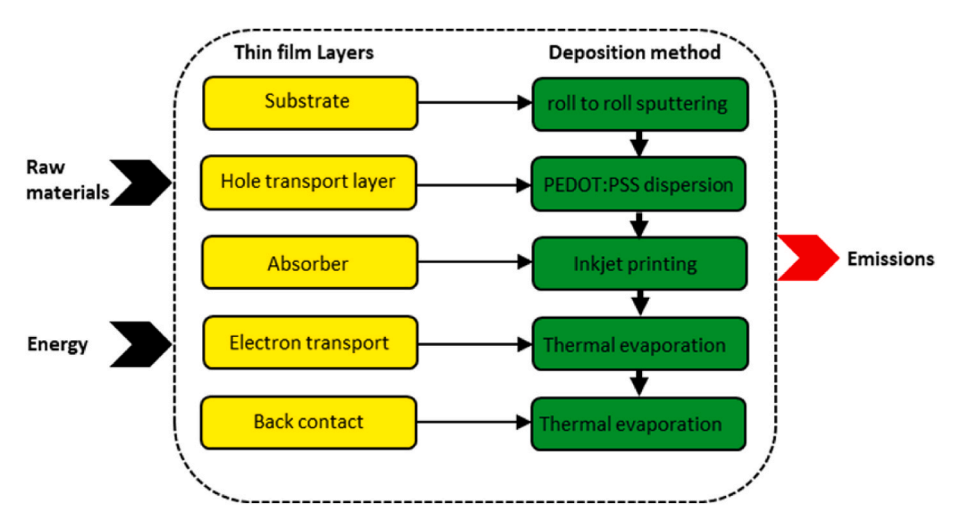


Fig. 1. System boundary for the cradle to gate life cycle assessment of the analysed perovskite solar cell.

evaporation of the hole transporting layer, and silver used as the back contact. The energy required for thermal evaporation of C60 used as the electron transport layer was calculated assuming the same equipment used for the deposition of the silver electrode. Thermal evaporator systems usually require the creation of a vacuum before evaporation and cooling after it has occurred (García-Valverde et al., 2010). Therefore, it was assumed that the energy for the vacuum pump and cooling system remained constant while the energy required to heat the filament of the evaporator was proportionally allocated to the electron transport layer based on the mass of C60. This was also assumed to be the energy required to deposit the bathocuproine buffer layer. Due to lack of data, complex chemicals used in the hole transporting layer, absorber layer, and back contact were obtained using the stoichiometric ratio of the chemicals or relevant literature. This includes PEDOT:PSS for the hole transporting layer, all chemicals except γ -butyrolactone for the absorber layer, and bathocuproine used in the back contact.

The environmental impact of indium used in the substrate and silver used as the back contact was calculated using the economic allocation method described in the Nuss and Eckelman (2014). The associated environmental impacts were calculated based on the five year average market price of different metals. The average market price of indium and silver between 2016 and 2020 was \$374.6/kg and \$558/kg, respectively, calculated from the database of the United State Geological Survey (USGS, 2021). The economic allocation was based on indium and silver obtained from zinc and copper processing, respectively.

2.3. Life cycle impact assessment

Appropriate life cycle impact assessment methods were used to allow for a full range of most relevant indicators to be included in the analysis. The indicators have been disaggregated into three main categories of environmental, human toxicity, and energy indicators. CML2001 method is highly relevant when assessment of metal depletion is being considered and it is the most used impact assessment method when the environmental impact of solar cells are being analysed (Muteri et al., 2020). In addition, ILCD2011 impact method was used to investigate the human toxicity indicators in more detail. Cumulative Energy Demand (CED) was used for detailing energy contributions (Table 5). For conversion to a single unit and for better comparison of results, a series of environmental impact category normalisations were performed. The results associated with CML2001 impact method were normalised based on CML 2001- Jan 2016 (CML - Department of Industrial Ecology, 2016) using EU25 + 3 factors. Human toxicity results of the ILCD2011 impact method were converted to DALY (Disability adjusted life years) using the normalisation factor found in (Huijbregts et al., 2005).

2.4. Sensitivity analysis

The results and discussions section includes sensitivity analyses covering the impact of a) the deposition method, and b) the precursor ink material used for the manufacturing of the perovskite. The results from spin coating as the most commonly used deposition method and inkjet printing as a promising emerging technique have been compared to identify their environmental contribution to the manufacturing of PSCs. Three precursor inks including a non-toxic green solvent used in Wilk et al. (2021), and two conventional inks used in Sarialtin et al. (2020) referred to as Ink-1, and used in Gong et al. (2015) referred to as Ink-2 were compared with respect to their environmental impacts as detailed in Tables 4 and 6. These inks were selected as they contained the most frequently used solvent for perovskite deposition, N, N-dimethylformamide (DMF) (Noel et al., 2017). Ink-2 differed from Ink-1 as it made use of isopropanol as an additional solvent for Methylammonium iodide as well as having much lower quantities of lead (II) iodide, hence a reduction in the environmental effect of the toxic chemical lead is expected (Gong et al., 2015).

Table 6 shows the life cycle inventory of Ink-1 and Ink-2 capable of

Table 5
Impact categories assessed with the CML 2001(Dreyer et al., 2003), ILCD2011 (EC-JRC, 2012), and cumulative energy demand(Frischknecht et al., 2015) (CED) methods with their abbreviations and characterisation units (Guinée, 2001).

Category		Impact method	Abbreviation	Unit
Environmental Impact Indicators	Abiotic depletion Abiotic depletion (fossil fuels)	CML2001	ADP ADPF	kg Sb eq MJ
	Global warming Ozone layer depletion		GWP ODP	kg CO ₂ eq kg CFC-11 eq
	Fresh water aquatic ecotoxicity		FWE	kg 1,4-DB eq
	Marine aquatic ecotoxicity		MAE	kg 1,4-DB eq
	Terrestrial ecotoxicity		TE	kg 1,4-DB eq
	Photochemical oxidation		POP	kg C ₂ H ₄ eq
	Acidification		AP	kg SO ₂ eq
Human Health Indicators	Eutrophication Human toxicity		EP HT	kg PO ₄ eq kg 1,4-DB eq
	Human toxicity with carcinogenic effect	ILCD2011	НТс	$\begin{array}{c} DALY/\\ kgC_2H_3Cl_{eq} \end{array}$
	Human toxicity without carcinogenic effect		HTnc	DALY/ kgC ₂ H ₃ Cl _{eq}
Energy Indicators	Primary energy non- renewable resource	CED	PENRT	MJ
	Primary energy renewable resource		PERT	MJ

producing absorber layers of PSCs to achieve the functional unit (1 kWh) using inkjet printing. Spin coating deposition method was modelled assuming 95% of the ink ending up as waste and not making it to the absorber layer. This is in line with the material loss (95–98%) observed in literature when spin coating is applied (Sahu et al., 2009). The energy requirement for spin coating (1.8 $\rm MJ/m^2$) was obtained from the work of Sarialtin et al. (2020) with post treatment assumed to be the same for both analysed deposition methods.

3. Results and discussion

The results and discussion section presents the impact assessment results of the studied PSCs. A sensitivity analysis section is included to compare the LCA results of the non-toxic green solvent precursor ink and inkjet printing deposition methods with inks containing the toxic compounds DMF and the spin coating.

3.1. Impact assessment of perovskite solar cells using relevant indicators

The impact assessment results of PSC solar cells is divided and presented in three sections. The first section highlights the environmental impact from materials and energy used in the manufacturing of the cells. The second and third sections present and discuss environmental impact results from each PSCs manufacturing layer and the composition of the green solvent perovskite ink respectively.

3.1.1. Impacts from materials and energy

The environmental impact profiles of the assessed PSCs were calculated by combining the considered process model assumptions, LCIs, and characterisation factors of the impact assessment methods. Table 7

Table 6LCI of two conventional perovskite absorber precursor inks producing 1 kWh of energy through inkjet printing.

Ink-1			Ink-2	Ink-2		
Input	Amount	Unit	Input	Amount	Unit	
Lead (II) iodide N,N-dimethylformamide Methylammonium iodide	0.33 0.46 0.11	mg mg mg	Lead (II) iodide N,N-dimethylformamide Methylammonium iodide Isopropanol	0.045 0.091 0.0046 0.36	mg mg mg mg	

Table 7Life cycle impact assessment results for Perovskite solar cell (impact per kWh).

Perovskite Solar Cell	Perovskite Solar Cell					
Impact indicators	Impact Category	Unit	Electricity	Manufacturing Materials		
Environmental	ADP	kg Sb eq	1.48E-08	1.75E-06		
Impact Indicators	ADPF	MJ	4.94E-01	1.20E-01		
	GWP	kg CO ₂ eq	4.40E-02	4.58E-03		
	ODP	kg CFC- 11 eq	1.42E-15	3.12E-16		
	FWE	kg 1,4- DB eq	1.92E-03	5.85E-05		
	MAE	kg 1,4- DB eq	9.66E-05	7.52E-01		
	TE	kg 1,4- DB eq	5.16E+00	5.88E-05		
	POP	kg C ₂ H ₄ eq	5.15E-05	1.99E-06		
	AP	kg SO ₂	6.26E-06	1.83E-05		
	EP	kg PO ₄	8.63E-05	1.29E-06		
Human Toxicity Indicators	HT	kg 1,4- DB eq	1.02E-05	9.93E-04		
	НТс	DALY	7.91E-01	1.02E-07		
	HTnc	DALY	3.65E-01	9.40E-07		
Energy Indicators	PENRT	MJ	1.48E-08	1.27E-01		
	PERT	MJ	4.94E-01	9.42E-03		

presents the impact assessment results categorised into electricity consumed and materials used to manufacture the cell in relation to the defined functional unit (1 kWh).

Fig. 2 demonstrates the individual material contributions to the selected impact categories of the CML2001 characterisation method. Materials used contributed significantly to HT (34.08%), ADP (99.16%), FWE (37.71%), TE (53.29%), and POP (24.08%) mainly due to the use of silver as the back contact. Silver was responsible for the majority of the impact from materials used in the ADP, HT, FWE, TE, and POP impact categories. It also contributed considerably in all other impact categories

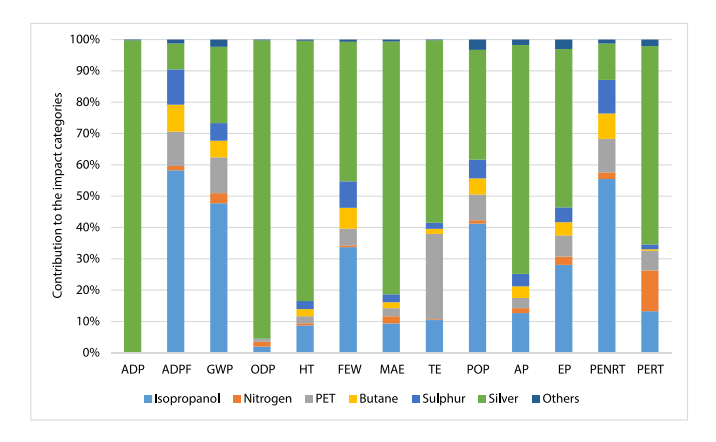


Fig. 2. Contribution of the manufacturing materials to the impact categories of Perovskite solar cell (impact per kWh).

including a quarter of the GWP from manufacturing materials. Isopropanol used for substrate cleaning and PET in the front contact also played a major role in the environmental impact of materials used in TE (isopropanol 10.43%; PET 27.23%), FWE (isopropanol 33.75%; PET 5.32%), and POP (isopropanol 41.23%; PET 8.21%) impact categories.

Electricity consumption contributed the highest in the majority of impact categories studied including ADPF, GWP, ODP, HT, FWE, MAE, POP, AP, EP, PENRT, and PERT (Table 7).

Apart from the environmental impact of PSCs, it is paramount that the effects of its production be assessed from an occupational health and safety perspective. This is due to numerous potentially toxic materials being used in the manufacturing of the cell. Many LCA studies carried out on solar panels have been lacking in this aspect as they primarily focus on environmental impacts without considering the potential negative effects of materials to humans (Bakhiyi et al., 2014). In the analysed cell, lead compounds such as lead acetate, lead bromide, and lead iodide have been identified as carcinogens to humans as they are classified under group 2A by the international agency for research on cancer (IARC) (International Agency For Research On Cancer, 2021). Lead (Agency for Toxic Substances And Disease Registry, 2021b), a raw material for the production of these chemicals is also a known carcinogen affecting both the digestive and central nervous system of humans (Bakhiyi et al., 2014). Alongside lead and lead compounds, materials such as zinc, iodine, and silver have some non-carcinogenic effect if introduced into the human body. Zinc (Agency for toxic substances and disease registry, 2021d) and silver (Agency for toxic substances and disease registry, 2021c) for instance negatively affect the digestive and respiratory system while iodine (Agency for Toxic Substances And Disease Registry, 2021a) targets the endocrine system. Silver, used as the back contact, is especially concerning as in the analysed cell it was found to cause around a quarter (3.30E-04 Kg 1,4-DB eq) of the impact in the HT impact category. Substituting silver for carbon black as the counter electrode may reduce its environmental impact (Sarialtin et al., 2020; Gong et al., 2015). The elimination of the commonly used toxic chemical N,N-dimethylformamide (DMF) for perovskite deposition in the assessed cell is beneficial as the compound is on the European Chemical Agency list of substances with very high concern (Vidal et al., 2021a). As PSCs are on the verge of mass production, elimination/minimisation of these potentially harmful materials need to be considered. Plant workers would need to undergo training on appropriate handling techniques and instructed to wear appropriate personal protective equipment.

This study found electricity consumption to be the main contributor to the environmental footprint of the assessed PSCs. The Energy Payback time (EPBT) in the context of CED in therefore determined. EPBT is the amount of time required for the PSCs to produce the energy equivalent of that used to manufacture them including the material embodied energy and the electricity consumption (Yousef and Hassan, 2020). The total electricity consumed to produce PSCs using inkjet printing for the functional unit (1 kWh) is 0.4023 MJ (0.1117 kWh) (see Table 4). The EPBT on that basis would be around 26 months (1 kWh of electricity, over 20 years service life, offsets the manufacturing energy in 2 years). This is similar to those observed in commercially available thin film solar cells such as CIGS and CdTe (Celik et al., 2018) suggesting that PSCs could potentially compete with these cells environmentally if scaled up. EPBT could be reduced if the assessed cell achieves a higher efficiency. Efficiencies as high as 25.7% have been observed in PSCs

deposited using spin coating, exceeding those seen in the commercially available CIGS which has efficiencies up till 23.4% (Kim et al., 2020). The EPBT of the assessed PSC reduces by more than 50% (12 months) if it had an efficiency of 25.7%, bettering those seen in CIGS and CdTe (Celik et al., 2018). EPBT could be further shortened by substituting materials having high embodied energy with lower impact alternatives. The use of isopropanol (52.56%) during substrate cleaning and silver (15.19%) as the back contact contributes significantly to CED in terms of materials used. Alternatives such as carbon black as the back contact coupled with reducing the reliance on isopropanol could reduce the embodied energy of the assessed PSC material and hence its EPBT.

It is also important to ascertain the relative magnitude of the impact categories to better understand the LCA results. Fig. 3 demonstrates the normalised emission factor per functional unit for the assessed environmental impact categories. MAE is the highest contributor to the environmental impacts after normalisation as it is around 6 times higher than the next significant impact category (ADPF). MAE measures the impact of toxic substances on marine ecosystem and is known to be caused by fluoride from electricity generation (Ozturk and Dincer, 2020). In this study, around 87% of the impact from this category comes from electricity consumption. Silver usage was the highest contributor when only manufacturing materials were taken into account (80.67% of the overall material impact).

3.1.2. Impacts from each manufactured layer

The environmental impact for each manufactured layer used to produce the assessed PSC analysed in more detail in this section and presented in Fig. 4. The hole transporting layer was found to have the highest impact in all the selected impact categories except TE with the absorber layer contributing the least to all the selected impact categories. Analysing the GWP contributions, production of the hole transporting layer was found to constitute 66.62% of its overall impact with the back contact, front contact, electron transport layer, and absorber contributing 19.24%, 6.76%, 4.42%, and 2.96% respectively. The high environmental impact seen in the hole transporting layer was due to the layer using 72% (0.2904 MJ) of the total electricity requirement of the assessed PSC. Alongside the hole transporting layer, the back contact made of silver was also a significant contributor to the overall environmental profile of the cell. Silver contributed the second highest in all impact categories except ADP (99.04%) where it contributed the highest. The front contact was found to considerably contribute to the ADPF, FEW, TE, POP, and PENRT categories as it recorded 14.51%, 15.54%, 20.72%, 12.90%, and 10.26% in these impact categories respectively. This was due to the use of isopropanol and PET in the manufacturing of the layer. The electron transport and perovskite absorber layers contributed <5% in all the selected impact categories. This suggests that the primary focus in reducing the environmental impact of the assessed cells should not be the absorber layer as is found in other thin-film technologies such as CIGS and CZTS (Collier et al., 2014). This is

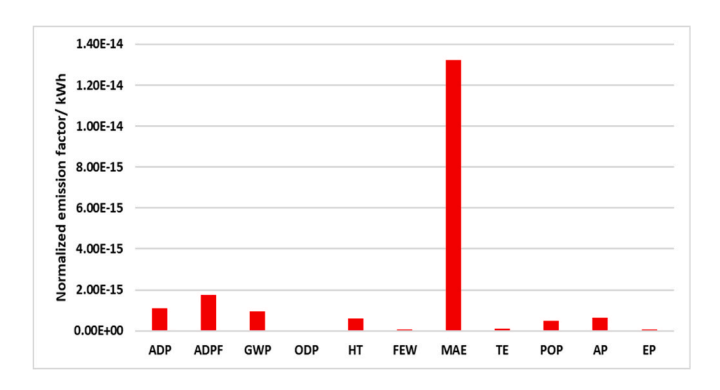


Fig. 3. Normalised emission factor for each assessed environmental impact category.

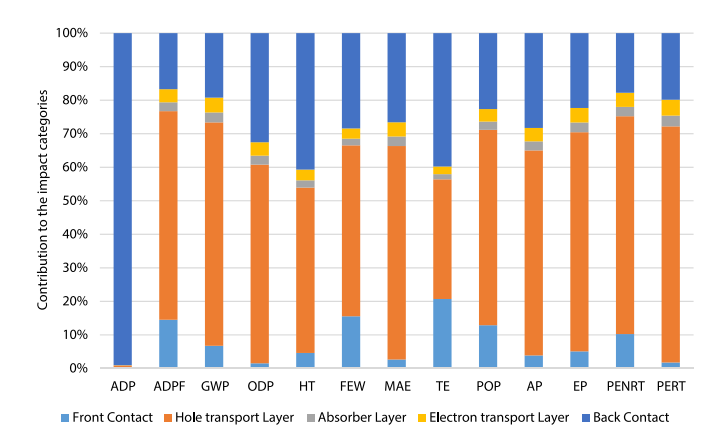


Fig. 4. Contribution to impact categories for the production of Perovskite solar cell (impact per kWh).

especially the case when the absorber layer is manufactured using low energy consuming techniques such as inkjet printing. Sarialtin et al. (2020) obtained similar results with regards to their absorber layer as the Fluorine doped tin oxide glass substrate contributed more than half to the environmental impact of hole transport free PSCs. Overall, the results demonstrate that the hole transport layer and the back contact material are the primary environmental hotspots and further design optimisations need to focus on these layers. Solutions such as eliminating the hole transport layer have already been developed and presented in the literature (Sarialtin et al., 2020).

3.1.3. Impacts from the perovskite precursor ink

The environmental impact of the perovskite precursor ink produced using green solvent was assessed in this study to determine its environmental profile in terms of compounds involved in its formulation. This was carried out to determine if a shift away from the toxic solvent DMF has a positive effect on reducing the environmental impacts.

Fig. 5 displays the environmental profile of the perovskite precursor ink produced using green solvents. The solvent γ -butyrolactone contributed the highest in the ADPF, GWP, HT, FEW, MAE, TE, POP, EP, PENRT, and PERT impact categories with Dimethyl sulfoxide and PbI2 contributing the highest in the ODP, and ADP and AP impact categories respectively. Formamidinium iodide is also a significant contributor to the ADP impact category following the PbI2. The chemical 2-methylpyrazine contributed considerably to the ADPF, FEW, TE, and PENRT and was the second highest in these categories. PbI2 (GWP, HT, MAE, POP, EP, and PERT) and formamidinium iodide (ADP and OD) contributed the second highest in the remaining impact categories. Cesium iodide contributed 5.92% to ADP with negligible contributions in the remaining impact categories. Formic acid and thiosemicarbazide contributed <2% in all the selected impact categories with methylammonium

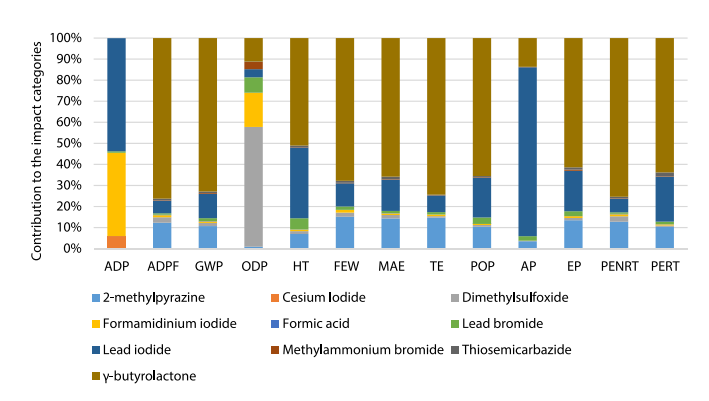


Fig. 5. Contribution to impact categories for the production of the perovskite precursor ink (impact per kWh).

bromide showing the same trend except in OD where it has a contribution of 3.37%.

As mentioned above, environmental impact results for the green solvent-based precursor ink used in this study was compared with two commonly used precursor inks in the literature. These are based on DMF, lead iodide, and methylammonium iodide for Ink-1 and Ink-2. These results are presented separately in Fig. 6 and Fig. 7 respectively and compared with the green solvent-based ink results in Table 8.

Fig. 6 demonstrated that Lead iodide is the environmental hotspot if Ink-1 with the highest impact in majority of the impact categories investigated (ADP, HT, FEW, MAE, TE, POP, AP, EP, PERT) due to the presence of lead in its chemical composition. DMF accounted for the highest impact in ADPF, GWP, and PENRT and second highest in HT, FEW, MAE, TE, POP, EP, and PERT. Methylammonium iodide had the lowest environmental impact in majority of the studied categories (less than 6%) and highest in ODP and significant in ADP.

The values associated with the use of Ink 2 (Fig. 7) demonstrate that Isopropanol is the environmental hotspot of this precursor ink accounting for the highest impact in majority of the impact categories (ADPF, GWP, HT, FEW, MAE, TE, POP, EP, PENRT, and PERT). Lead iodide follows isopropanol with the highest impact in ADP and AP and second highest in ODP, HT, MAE, POP, EP, and PERT. Methylammonium iodide shows the highest impact in ODP and a considerable role in ADP. DMF accounts for the second highest in ADPF and PENRT, and a significant contributor to GWP, MAE, EP, and PERT.

Ink-2 performs better environmentally in all impact categories when directly compared with Ink-1. This is mainly related to the lower quantity of lead iodide, DMF, and methylammonium iodide used in it composition due to the presence of isopropanol.

A normalisation study was applied to the results similar to the previous sections to allow for a single-unit comparison between the impact categories. These results are displayed in Fig. 8 for the green perovskite precursor ink, Ink-1, and Ink-2.

The ADP impact category has the highest magnitude when compared with other environmental impact categories. ADP is the reduction in the availability of abiotic natural resources and its relatively high environmental impact is due to the presence of lead iodide in all the inks (Van Oers and Guinée, 2016). The quantity however in the assessed green perovskite precursor ink (1.74E-06 mg) is significantly lower than that found in both Ink-1 (0.33 mg) and ink 2 (0.045 mg). Another major contributor to the ADP impact category is formamidinium iodide in our assessed ink and Methylammonium iodide found in Ink-1 and Ink-2.

3.2. Sensitivity analysis

The sensitivity analysis is divided into two sections. The first section compares the green solvent perovskite precursor ink with ink 1 and 2 which contains the toxic chemical DMF. The second section compares inkjet printing deposition method with that of spin coating.

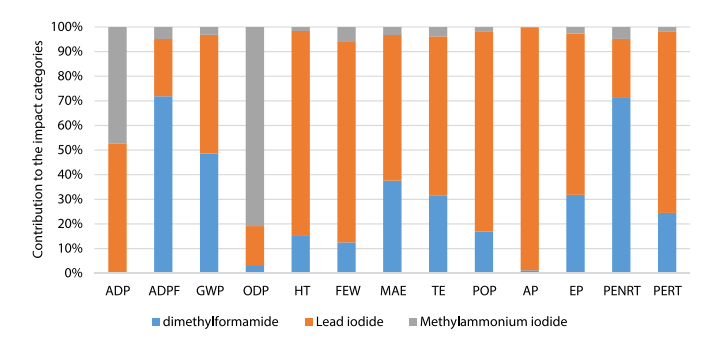


Fig. 6. Contribution to impact categories for the production of perovskite precursor Ink-1 (impact per kWh), Inventory obtained from Sarialtin et al. (Sarialtin et al., 2020).

3.2.1. Precursor inks

Further comparative analysis between the green solvent-based precursor ink and the two other ink compositions is demonstrated in Table 8. This clearly demonstrates the significant environmental benefit of switching to PSCs produced using the assessed green-solvent based precursor inks. The values associated with the green solution are significantly lower in all impact categories demonstrating promising potential for their integration with future PSCs developments.

3.2.2. Deposition methods: inkjet printing vs spin coating

The inkjet printing was compared environmentally with the most commonly reported deposition method, spin coating (Table 9). Inkjet printing demonstrates better environmental performance than spin coating. This is mainly due to 95% of the ink being wasted during the spin coating process. This figure for the inkjet printing is a near 0% waste production. The required energy for spin coating and inkjet printing are 1.8 MJ/m² (Sarialtin et al., 2020) and 1.152 MJ/m², respectively, demonstrating a 36% reduction in energy consumption for inkjet printing (both methods require a post treatment energy demand of 0.792 MJ/m²). Inkjet printing deposition method has the added advantage of being able to be deployed on a commercial scale. Other scalable deposition methods such as drop casting, doctor blade coating, slot die coating, and spray coating also have industrial scalability potential. The benefit of using inkjet printing over these methods is the lower relative ink volume required due to minimal ink wastage. Careful selection of the precursor ink alongside deploying adequate post treatment of the perovskite film can reduce the environmental impact of PSCs significantly. Another challenge associated with inkjet printing that may limit its adoption is controlling the accuracy of the printer jetting nozzle (Li et al., 2021) which will require further investigation.

The results obtained in this study were compared with available studies (per m²) assessing the environmental impacts of PSCs using other deposition methods. The MAE impact category which was identified after normalisation as having the highest magnitude compared to other categories could not be adequately compared with literature. This is due to different impact characterisation methods used by the identified LCA studies. GWP and CED were therefore used as proxies for environmental impact comparison as two of the most commonly used proxies in the literature although not reflecting the most impactful categories as identified in this study. Table 10 demonstrates significant environmental benefits for inkjet printing presenting a lower GWP and CED values (GWP: 7.54 kg CO₂eq/m²; CED: 200.18 MJ/m²) compared with other deposition methods. The most commonly used deposition method, spin coating had a median GWP and CED value of 74.5 kg CO₂eq/m² and 1204 MJ/m² respectively. This was relatively low when compared with other energy intensive methods like vapour (GWP: 1148 kg CO₂eq/m²; CED: $10,827 \text{ MJ/m}^2$) and vacuum (GWP: $188 \text{ kg CO}_2\text{eq/m}^2$; CED: 3040MJ/m²) deposition methods. This better environmental performance of inkjet printed PSCs, coupled with the technology's potential for industrial scale-ups, suggest a promising future for the technology.

4. Summary and limitations of study

In this paper, for the first time, a cradle-to gate life cycle assessment of inkjet printed PSCs were performed. The analysis included an assessment of a novel green solvent based perovskite precursor ink using manufacturing procedures developed recently. A special focus was given to investigating the environmental benefits of eliminating conventional toxic solvent materials used in applying the perovskite layer. Different impact categories (ADP, TE, ADPF, GWP, ODP, HT, FWE, MAE, POP, AP, EP, PENRT, and PERT) were selected to assess the environmental performance using a functional unit of 1 kWh. The results of the comprehensive LCA study demonstrated that environmental and toxicology impacts from the use of electricity is by far the largest for PSCs production contributing the highest in majority of the impact categories. Manufacturing materials used were the major contributor to the ADP

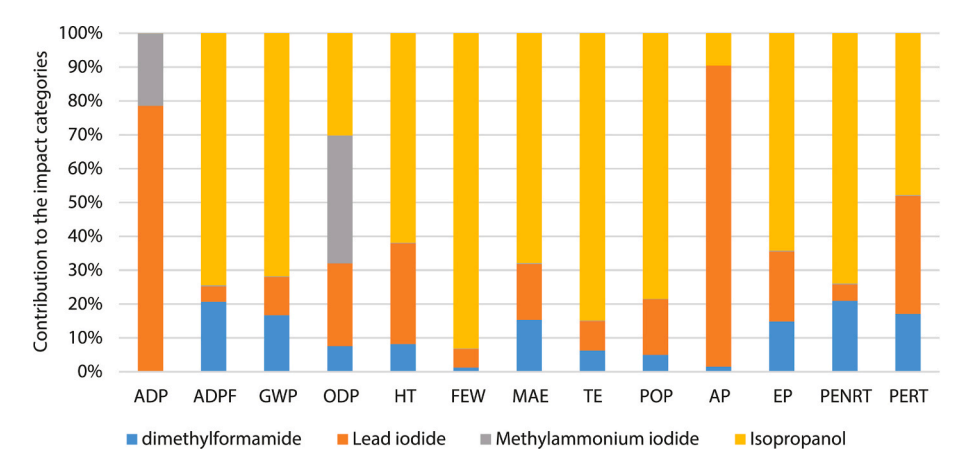


Fig. 7. Contribution to impact categories for the production of perovskite precursor Ink-2 (impact per kWh), Inventory obtained from Gong et al. (Gong et al., 2015).

Table 8Comparison of the life cycle impact assessment results of different perovskite precursor inks (impact per kWh).

<u>'</u>		Perovskite Precursor Ink		
Impact Category	Unit	Green	Ink-1	Ink-2
ADP	kg Sb eq	4.93E-14	9.53E-08	8.58E-09
ADPF	MJ	7.78E-10	3.78E-04	2.63E-04
GWP	kg CO ₂ eq	3.23E-11	1.47E-05	8.50E-06
ODP	kg CFC-11 eq	1.44E-24	6.68E-19	5.83E-20
HT	kg 1,4-DB eq	1.37E-12	1.05E-06	3.95E-07
FWE	kg 1,4-DB eq	1.17E-13	2.98E-08	5.95E-08
MAE	kg 1,4-DB eq	1.26E-09	5.95E-04	2.90E-04
TE	kg 1,4-DB eq	9.03E-14	2.02E-08	2.02E-08
POP	kg C ₂ H ₄ eq	9.95E-15	4.38E-09	2.93E-09
AP	kg SO ₂ eq	2.95E-13	4.55E-07	6.83E-08
EP	kg PO ₄ eq	6.70E-15	3.70E-09	1.58E-09
PENRT	MJ	7.98E-10	4.28E-04	2.90E-04
PERT	MJ	4.70E-11	2.58E-05	7.35E-06

(99.16%) and TE (53.29%) impact categories, also having significant contributions to HT (34.08%), FWE (37.71%) and POP (24.08%). This was mainly due to the use of silver as the back contact. Isopropanol used for substrate cleaning and PET in the front contact also played a major

role in the environmental impact of materials used. MAE was found to have the highest magnitude of all the selected impact categories after normalisation with electricity consumption contributing 87% to the impact category.

When each manufactured layer was assessed, it was discovered that

Table 9The LCIA results of the green precursor ink deposited using inkjet printing and Spin coating (impact per kWh).

Impact Category	Unit	Inkjet Printing	Spin coating
ADP	kg Sb eq	4.85E-10	6.15E-10
ADPF	MJ	1.61E-02	2.05E-02
GWP	kg CO2 eq	1.44E-03	1.83E-03
ODP	kg CFC-11 eq	4.63E-17	5.88E-17
HT	kg 1,4-DB eq	6.28E-05	7.95E-05
FWE	kg 1,4-DB eq	3.15E-06	4.00E-06
MAE	kg 1,4-DB eq	1.68E-01	2.14E-01
TE	kg 1,4-DB eq	1.68E-06	2.13E-06
POP	kg C2H4 eq	2.05E-07	2.60E-07
AP	kg SO2 eq	2.80E-06	3.58E-06
EP	kg PO4 eq	3.33E-07	4.20E-07
PENRT	MJ	2.58E-02	3.28E-02
PERT	MJ	1.19E-02	1.51E-02

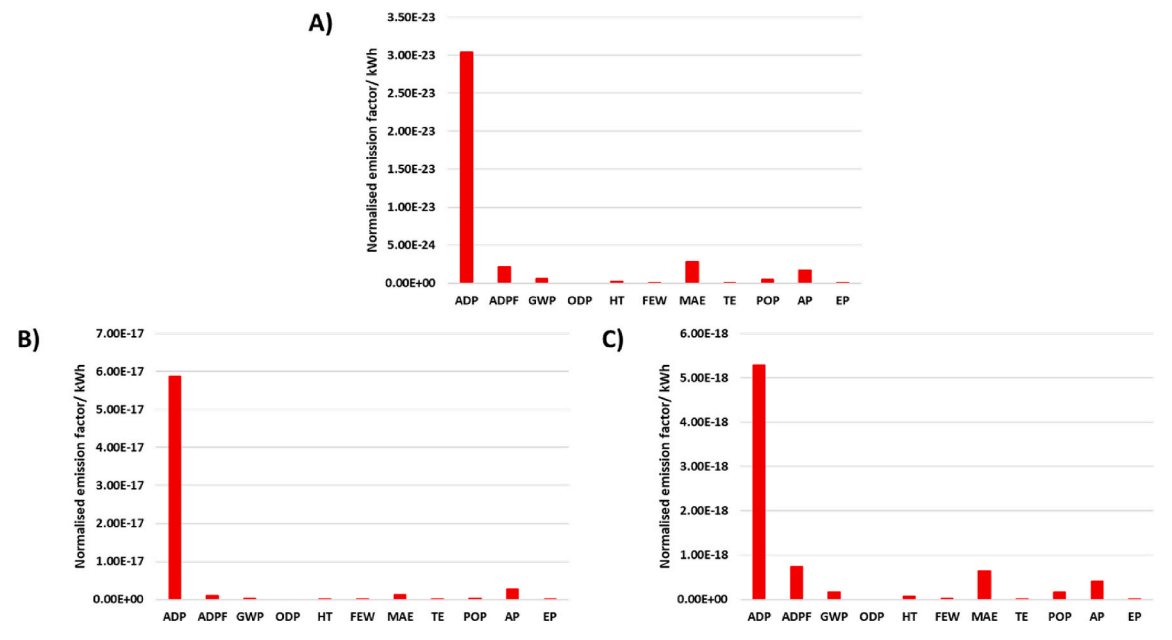


Fig. 8. Normalised emission factor for the environmental impact categories of A) Green perovskite precursor ink B) Ink-1 and C) Ink-2.

Table 10
Comparison of the GWP and CED of life cycle assessment studies on PSCs (Adapted from Vidal et al. (2021b)).

Active Layer	Deposition Method	Efficiency (%)	GWP (kg CO ₂ eq/ m ²)	CED (MJ/ m ²)	References
Cs _{0.1} [(HC(NH ₂) ₂) _{0.83} (CH ₃ NH ₃) _{0.17}] _{0.9} Pb (I _{0.83} Br _{0.17}) ₃	Inkjet printing	11.4	7.54	200.18	This Study
MAPbI ₃	Spin-coating 1:3	11.4	57	1055	(Alberola-Borràs et al.,
MAPbI ₃	Spin-coating 1:1	10.4	58	1060	2018a)
MAPbI ₃	Spin-coating + dipping	15	78	1489	
MAPbI ₃	Spin-coating	12.3	75	1348	
	Spin-coating	_	_	_	
$MAPbI_3$	Screen printing	11	33	724	
MAPbI ₃	Spin-coating 1:1	19	74	1667	
MAPbI ₃	Spray	15	157	2550	Celik et al. (2016)
MAPbI ₃	Vacuum deposition	15	188	3040	
$MAPbI_3$	Spray	15	127	2070	
PbCl ₂ /CH ₂ NH ₃ I	Spin-coating	11.5	819	9149	
PbCl ₂ /CH ₂ NH ₃ I	Spin coating	11.4	795.0	_	
$MAPbI_3$	Spin-coating + dipping	11	19	400	
Pb-based perovskite	Spin coating	9.1	10	_	
Pb-based perovskite	Thermal co evaporating	15	200	_	
Pb-based perovskite	Spray coating	15	175	_	
$Cs_{(x)}FA_{(1-x)}PbI_{(3-y)}Br_{y}$	Spin-coating	21.1	45	501	Ibn-Mohammed et al.
MAPbI ₃	Vapour deposition	15.1	52	721	(2017)
$MAPbI_3$	Thermal evaporation and slot die	13.8	102	1185	
Pb-based perovskite	Thermal evaporation of Pbl ₂ and slot die coating of MAI	18.3	175	-	
Pb-based perovskite	Spin coating	6.5	1650	_	
MAPbI ₃	Spin-coating + dipping	6.5	286	10,080	
$MAPbI_3$	Spin-coating	11.5	45	741	
$MAPbI_3$	Spin-coating	14.5	45	744	
CH ₃ NH ₃ SnI ₃	Spin-coating	6.4	931	9009	
PbCl ₂ /CH ₃ NH ₃ I	Vapour deposition	15.4	1148	10,827	
Pb-based perovskite	Thermal co-evaporation	15.4	1147	_	
Pb-based perovskite	Spin-coating	11.5	785	_	

the main contributor to the overall environmental impact was the hole transporting layer. This was attributed to the layer being responsible for 72% of the overall energy requirement of the evaluated PSC. Analysis of only the absorber layer revealed that it contributed less than 4% to all of the identified impact categories. This suggests that, unlike the absorber layers of other thin film cells such as CIGS and CZTS, the absorber layer of inkjet printed PSCs is not the primary contributor to the technology's environmental impact. For PSCs to realise their full environmental saving potentials, the focus should be on the hole transport layer, which has been identified as a hotspot, with the goal of lowering its energy consumption or eliminating it entirely. Hole transport layer-free devices have previously been produced.

Perovskite precursor ink produced using green solvents was also assessed with the same selected impact categories. The analysis showed that the presence of lead is significant as it contributed the most to ADP which after normalisation was found to have the highest magnitude of the selected impact categories. Other main contributors to the environmental impact of the ink were γ -butyrolactone, dimethylsulfoxide, formamidinium iodide, PbI_2, and co-solvent 2-methylpyrazine. When the assessed precursor ink was compared with other precursor inks containing the conventional solvent DMF, a better environmental performance was observed. Inkjet printed PSC when combined with less harmful precursor inks such as the precursor analysed in this study is expected to challenge existing solar cell technologies such as CIGS while revolutionising the industry.

The environmental assessment conducted in this study made use of parameters obtained from lab-based cells, as PSCs are currently not manufactured on an industrial scale. These values may deviate from those seen when industrial production processes are established for PSCs. Due to constant research and development of environmentally friendly deposition techniques and the drive to shift away from energy produced using fossil fuels, the environmental impact of real world large scale PSCs production process may be lower than those observed here. To remove uncertainties in the environmental assessment of PSCs, data

needs to be obtained from pilot scale operations. PSC is a relatively new technology, therefore, limited amounts of such operations are available. As the technology matures, PSCs may be able to overcome challenges regarding stability and longevity to be able to be manufactured on an industrial scale using deposition methods such as inkjet printing.

5. Conclusions

Perovskite solar cells (PSCs), one of the emerging novel technologies designated as third generation solar cells, have attracted considerable attention as a feasible alternative to existing solar cell technologies. This is due to the continual record-breaking power conversion efficiencies reported in the last decade. However, PSCs are still in the research and development and early commercialisation stages and have yet to be mass produced on a large scale. Inkjet printing, which was originally used for printed electronics, has recently been adapted to solar cell production and has shown promising upscaling potential. A great deal of work has been published on the technical feasibility of utilising inkjet printing however, their environmental performance has not been investigated.

This paper assessed, for the first time, the environmental impact of producing inkjet printed PSCs contributing to the full assessment of utilising inkjet printing as a scalable technology. Using a novel green solvent based perovskite precursor ink developed recently by the authors, the paper also addressed the concerns associated with the toxicity of the solvents utilised in the PSC production. The extensive analyses in the paper highlighted that the electricity consumed during the manufacturing of the cell had the highest environmental impact in the majority of the impact categories. This further highlights the need for moving towards decarbonising the grid. Materials contributed significantly to ADP and TE primarily due to the use of silver as the back contact, comparing the green solvent based precursor ink with two other precursor inks containing the conventional solvent N,N-dimethylformamide, indicated that the green ink performed better

environmentally although the use of lead was found to be a major issue for all three material configurations.

This research provides important environmental insights for product design optimisation and material configuration by highlighting their environmental hotspots. The work lays the groundwork for further research into PSC's environmental profile and long-term viability. This work could be expanded to a cradle to grave assessment on inkjet printing deposition method when data on the in-use and end-of-life phases become available as the technology matures. To complement the environmental assessment, comprehensive life cycle costing analysis needs to be conducted in order to adequately compare costs with commercially available solar cells, compiling all effective parameters informing the decision making process. A number of other challenges, such as increasing renewable energy use and reducing the reliance on toxic materials and expensive noble metals need to be overcome in order to move PSCs from a laboratory scale to the large-scale industrial production.

CRediT authorship contribution statement

Tobechi Okoroafor: Data curation, Writing – original draft, Software. **Amani Maalouf:** Methodology, Investigation. **Senol Oez:** Conceptualization, Validation. **Vivek Babu:** Validation, Writing – review & editing. **Barbara Wilk:** Validation, Conceptualization. **Shahaboddin Resalati:** Conceptualization, Methodology, Writing – review & editing, Supervision.

Declaration of competing interest

The authors declare that they have no known competing financial interests or personal relationships that could have appeared to influence the work reported in this paper.

Data availability

Data will be made available on request.

Acknowledgments

This project has received funding from the European Union's Horizon 2020 research and innovation programme under grant agreement No 869898.

Abbreviations

ADP Abiotic depletion

PEDOT:PSS poly (3,4ethylenedioxythiophene) polystyrene sulfonate

Mono-Si Monocrystalline silicon Multi-Si Polycrystalline silicon a-Si Amorphous silicon

ADPF Abiotic depletion (fossil fuels)

AP Acidification

HCL

CED Cumulative energy demand

CdTe Cadmium telluride

CIGS Copper indium gallium selenide

C60 buckminsterfullerene DMAc *N*,*N*-dimethyl acetamide DMF *N*,*N*-dimethylformamide **DMSO** dimethyl sulfoxide EP Eutrophication **EPBT** Energy payback time Flash InfraRed Annealing **FIRA** FTO Fluorine-doped tin oxide **FWE** Freshwater aquatic ecotoxicity Global Warming Potential **GWP**

Hydrochloric acid

HT Human toxicity

HTc Human toxicity with carcinogenic effect HTnc Human toxicity without carcinogenic effect

IZO indium zinc oxide
ITO tin-doped indium oxide
LCA Life cycle assessment
MAE Marine aquatic ecotoxicity
NMP N-methyl-2-pyrrolidone
ODP Ozone layer depletion

PENRT Primary energy non-renewable resource
PERT Primary energy renewable resource

PET polyethylene terephthalate
POP Photochemical oxidation
PSCs Perovskite solar cells
PTAA Poly(triarylamine)
TE Terrestrial ecotoxicity

References

Agency for Toxic Substances And Disease Registry, 2021a. Toxicology profile for iodine [Online]. Available: https://wwwn.cdc.gov/TSP/substances/ToxSubstance.aspx?toxid=85. (Accessed 1 November 2021).

Agency for Toxic Substances And Disease Registry, 2021b. Toxicology profile for lead [Online]. Available: https://wwwn.cdc.gov/TSP/substances/ToxSubstance.aspx?toxid=22. (Accessed 1 November 2021).

Agency for toxic substances and disease registry, 2021c. Toxicology profile for silver [Online]. Available: https://wwwn.cdc.gov/TSP/substances/ToxSubstance.aspx?toxid=97. (Accessed 1 November 2021), 2021.

Agency for toxic substances and disease registry, 2021d. Toxicology profile for zinc [Online]. Available: https://wwwn.cdc.gov/TSP/substances/ToxSubstance.aspx?toxid=54. (Accessed 1 November 2021), 2021.

Alberola-Borràs, J.-A., Baker, J.A., De Rossi, F., Vidal, R., Beynon, D., Hooper, K.E.A., Watson, T.M., Mora-Seró, I., 2018. Perovskite photovoltaic modules: life cycle assessment of pre-industrial production process. iScience 9, 542–551.

Amarakoon, S., Vallet, C., Curran, M.A., Haldar, P., Metacarpa, D., Fobare, D., Bell, J., 2018. Life cycle assessment of photovoltaic manufacturing consortium (PVMC) copper indium gallium (di)selenide (CIGS) modules. Int. J. Life Cycle Assess. 23, 851–866

Ansari, M.I.H., Qurashi, A., Nazeeruddin, M.K., 2018. Frontiers, opportunities, and challenges in perovskite solar cells: a critical review. J. Photochem. Photobiol. C Photochem. Rev. 35, 1–24.

Bakhiyi, B., Labrèche, F., Zayed, J., 2014. The photovoltaic industry on the path to a sustainable future—environmental and occupational health issues. Environ. Int. 73, 224–234.

Celik, I., Philips, A.B., Song, Z., Yan, Y., Ellingson, R.J., Heben, M.J., Apul, D., 2018. Energy payback time (EPBT) and energy Return on energy invested (EROI) of perovskite tandem photovoltaic solar cells. IEEE J. Photovoltaics 8, 305–309.

Celik, I., Song, Z., Cimaroli, A.J., Yan, Y., Heben, M.J., Apul, D., 2016. Life Cycle Assessment (LCA) of perovskite PV cells projected from lab to fab. Sol. Energy Mater. Sol. Cell. 156, 157–169.

Cml - Depatment Of Industrial Ecology, 2016. In: ECOLOGY, C.-D.O.I. (Ed.), Cml-Ia Characterisation Factors.

Collier, J., Wu, S., Apul, D., 2014. Life cycle environmental impacts from CZTS (copper zinc tin sulfide) and Zn3P2 (zinc phosphide) thin film PV (photovoltaic) cells. Energy 74, 314, 321

Dreyer, L.C., Niemann, A.L., Hauschild, M.Z., 2003. Comparison of three different LCIA methods: EDIP97, CML2001 and Eco-indicator 99. Int. J. Life Cycle Assess. 8, 191–200.

EC-JRC 2012. Characterisation factors of the ILCD Recommended Life Cycle Impact Assessment methods. Database and Supporting Information. European Commission Joint Research Centre. Institute for Environment and Sustainability.

Espinosa, N., Serrano-Luján, L., Urbina, A., Krebs, F.C., 2015. Solution and vapour deposited lead perovskite solar cells: ecotoxicity from a life cycle assessment perspective. Sol. Energy Mater. Sol. Cell. 137, 303–310

Frischknecht, R., Wyss, F., Büsser Knöpfel, S., Lützkendorf, T., Balouktsi, M., 2015.

Cumulative energy demand in LCA: the energy harvested approach. Int. J. Life Cycle

Assess: 20, 057, 060

Fthenakis, V., Frischknecht, R., Raugei, M., Kim, H.C., Alsema, E., Held, M., De Wild-Scholten, M., 2011. Methodology Guidelines on Life Cycle Assessment of Photovoltaic Electricity. IEA PVPS Task, p. 12.

GaBi, 2022. GaBi LCA databases [Online]. Available: https://gabi.sphera.com/databases/gabi-databases/. (Accessed 22 May 2022), 2022.

García-Valverde, R., Cherni, J.A., Urbina, A., 2010. Life cycle analysis of organic photovoltaic technologies. Prog. Photovoltaics Res. Appl. 18, 535–558.

Gong, J., Darling, S.B., You, F., 2015. Perovskite photovoltaics: life-cycle assessment of energy and environmental impacts. Energy Environ. Sci. 8, 1953–1968.

Guinée, J., 2001. Life Cycle Assessment: an Operational Guide to the ISO Standards; LCA in Perspective; Guide; Operational Annex to Guide. Centre for Environmental Science, Leiden University, The Netherlands.

- Huijbregts, M.A., Rombouts, L.J., Ragas, A.M., Van De Meent, D., 2005. Humantoxicological effect and damage factors of carcinogenic and noncarcinogenic chemicals for life cycle impact assessment. Integrated Environ. Assess. Manag.: Int. J. 1. 181–244.
- Ibn-Mohammed, T., Koh, S., Reaney, I., Acquaye, A., Schileo, G., Mustapha, K., Greenough, R., 2017. Perovskite solar cells: an integrated hybrid lifecycle assessment and review in comparison with other photovoltaic technologies. Renew. Sustain. Energy Rev. 80, 1321–1344.
- International Agency For Research On Cancer, 2021. Agents classified by the IARC Monographs [Online]. Available: https://monographs.iarc.who.int/list-of-classifications. (Accessed 11 January 2021), 2021.
- International Organization For Standardization, 2006a. Environmental Management: Life Cycle Assessment; Principles and Framework. ISO.
- International Organization For Standardization, 2006b. Environmental Management: Life Cycle Assessment; Requirements and Guidelines. ISO Geneva, Switzerland.
- Itten, R., Stucki, M., 2017. Highly efficient 3rd generation multi-junction solar cells using silicon heterojunction and perovskite tandem: Prospective life cycle environmental impacts. Energies 10, 841.
- Jung, E., Budzinauskas, K., Öz, S., Ünlü, F., Kuhn, H., Wagner, J., Grabowski, D., Klingebiel, B., Cherasse, M., Dong, J., Aversa, P., Vivo, P., Kirchartz, T., Miyasaka, T., Van Loosdrecht, P.H.M., Perfetti, L., Mathur, S., 2020. Femto- to Microsecond Dynamics of excited electrons in a Quadruple cation perovskite. ACS Energy Lett. 5, 785–792.
- Kim, J.Y., Lee, J.-W., Jung, H.S., Shin, H., Park, N.-G., 2020. High-efficiency perovskite solar cells. Chem. Rev. 120, 7867–7918.
- Li, D., Zhang, D., Lim, K.-S., Hu, Y., Rong, Y., Mei, A., Park, N.-G., Han, H., 2021. A review on scaling up perovskite solar cells. Adv. Funct. Mater. 31, 2008621.
- Liang, X., Ge, C., Fang, Q., Deng, W., Dey, S., Lin, H., Zhang, Y., Zhang, X., Zhu, Q., Hu, H., 2021. Flexible perovskite solar cells: progress and prospects. Frontiers in Materials 8.
- Liu, Y., Akin, S., Hinderhofer, A., Eickemeyer, F.T., Zhu, H., Seo, J.-Y., Zhang, J., Schreiber, F., Zhang, H., Zakeeruddin, S.M., Hagfeldt, A., Dar, M.I., Grätzel, M., 2020. Stabilization of highly efficient and stable phase-pure FAPbI3 perovskite solar cells by molecularly tailored 2D-overlayers. Angew. Chem. Int. Ed. 59, 15688–15694.
- Maranghi, S., Parisi, M.L., Basosi, R., Sinicropi, A., 2019. Environmental profile of the manufacturing process of perovskite photovoltaics: harmonization of life cycle assessment studies. Energies 12, 3746.
- Monteiro Lunardi, M., Wing Yi Ho-Baillie, A., Alvarez-Gaitan, J.P., Moore, S., Corkish, R., 2017. A life cycle assessment of perovskite/silicon tandem solar cells. Prog. Photovoltaics Res. Appl. 25, 679–695.
- Muteri, V., Cellura, M., Curto, D., Franzitta, V., Longo, S., Mistretta, M., Parisi, M.L., 2020. Review on life cycle assessment of solar photovoltaic panels. Energies 13, 252.
- Noel, N.K., Habisreutinger, S.N., Wenger, B., Klug, M.T., Hörantner, M.T., Johnston, M. B., Nicholas, R.J., Moore, D.T., Snaith, H.J., 2017. A low viscosity, low boiling point, clean solvent system for the rapid crystallisation of highly specular perovskite films. Energy Environ. Sci. 10, 145–152.
- NREL, 2022. Best research-cell efficiency chart [Online]. Available: https://www.nrel.gov/pv/cell-efficiency.html. (Accessed 20 May 2022), 2022.
- Nuss, P., Eckelman, M.J., 2014. Life cycle assessment of metals: a scientific Synthesis. PLoS One 9, e101298.
- Ozturk, M., Dincer, I., 2020. Life cycle assessment of hydrogen-based electricity generation in place of conventional fuels for residential buildings. Int. J. Hydrogen Energy 45, 26536–26544.
- Resalati, S., Okoroafor, T., Maalouf, A., Saucedo, E., Placidi, M., 2022. Life cycle assessment of different chalcogenide thin-film solar cells. Appl. Energy 313, 118888.
- Roy, P., Kumar Sinha, N., Tiwari, S., Khare, A., 2020. A review on perovskite solar cells: Evolution of architecture, fabrication techniques, commercialization issues and status. Sol. Energy 198, 665–688.

- Sahu, N., Parija, B., Panigrahi, S., 2009. Fundamental understanding and modeling of spin coating process: a review. Indian J. Phys. 83, 493–502.
- Sánchez, S., Vallés-Pelarda, M., Alberola-Borràs, J.-A., Vidal, R., Jerónimo-Rendón, J.J., Saliba, M., Boix, P.P., Mora-Seró, I., 2019. Flash infrared annealing as a cost-effective and low environmental impact processing method for planar perovskite solar cells. Mater. Today 31, 39–46.
- Sarialtin, H., Geyer, R., Zafer, C., 2020. Life cycle assessment of hole transport free planar–mesoscopic perovskite solar cells. J. Renew. Sustain. Energy 12, 023502.
- Serrano-Lujan, L., Espinosa, N., Larsen-Olsen, T.T., Abad, J., Urbina, A., Krebs, F.C., 2015. Tin-and lead-based perovskite solar cells under scrutiny: an environmental perspective. Adv. Energy Mater. 5, 1501119.
- Speck, R., Selke, S., Auras, R., Fitzsimmons, J., 2016. Life cycle assessment software: selection can impact results. J. Ind. Ecol. 20, 18–28.
- Tilley, R.J., 2016. Perovskites: Structure-Property Relationships. John Wiley & Sons. Tu, Y., Wu, J., Xu, G., Yang, X., Cai, R., Gong, Q., Zhu, R., Huang, W., 2021. Perovskite solar cells for space applications: progress and challenges. Adv. Mater. 33, 2006545.
- Ünlü, F., Jung, E., Haddad, J., Kulkarni, A., Öz, S., Choi, H., Fischer, T., Chakraborty, S., Kirchartz, T., Mathur, S., 2020. Understanding the interplay of stability and efficiency in A-site engineered lead halide perovskites. Apl. Mater. 8, 070901.
- Ünlü, F., Jung, E., Öz, S., Choi, H., Fischer, T., Mathur, S., 2021. Chemical processing of mixed-cation hybrid perovskites: stabilizing effects of configurational entropy. https://doi.org/10.1002/9783527825790.ch1. Perovskite Solar Cells.
- USGS, 2021. Commodity statistics and information [Online]. Available: https://www.usgs.gov/centers/nmic/commodity-statistics-and-information#Z. (Accessed 30 April 2021), 2021.
- Van Oers, L., Guinée, J., 2016. The abiotic depletion potential: background, Updates, and future. Resources 5, 16.
- Vidal, R., Alberola-Borràs, J.-A., Habisreutinger, S.N., Gimeno-Molina, J.-L., Moore, D.T., Schloemer, T.H., Mora-Seró, I., Berry, J.J., Luther, J.M., 2021a. Assessing health and environmental impacts of solvents for producing perovskite solar cells. Nat. Sustain. 4 277–285
- Vidal, R., Alberola-Borràs, J.-A., Sánchez-Pantoja, N., Mora-Seró, I., 2021b. Comparison of perovskite solar cells with other photovoltaics technologies from the point of View of life cycle assessment. Adv. Energy Sustain. Res. 2, 2000088.
- Wang, Z., Jiang, Y., 2021. Advances in perovskite solar cells: film morphology control and interface engineering. J. Clean. Prod. 317, 128368.
- Wei, Z., Chen, H., Yan, K., Yang, S., 2014. Inkjet printing and instant chemical transformation of a CH3NH3PbI3/nanocarbon electrode and interface for planar perovskite solar cells. Angew. Chem. 126, 13455–13459.
- Wilk, B., Öz, S., Radicchi, E., Ünlü, F., Ahmad, T., Herman, A.P., Nunzi, F., Mathur, S., Kudrawiee, R., Wojciechowski, K., 2021. Green solvent-based perovskite precursor development for ink-jet printed flexible solar cells. ACS Sustain. Chem. Eng. 9, 3920–3930.
- Yousef, M.S., Hassan, H., 2020. Energy payback time, exergoeconomic and enviroeconomic analyses of using thermal energy storage system with a solar desalination system: an experimental study. J. Clean. Prod. 270, 122082.
- Zhang, J., Gao, X., Deng, Y., Li, B., Yuan, C., 2015. Life cycle assessment of titania perovskite solar cell technology for sustainable design and manufacturing. ChemSusChem 8, 3882–3891.
- Zhang, J., Wang, L., Jiang, C., Cheng, B., Chen, T., Yu, J., 2021. CsPbBr3 nanocrystal induced bilateral interface modification for efficient planar perovskite solar cells. Adv. Sci. 8, 2102648.
- Zhang, J., Zhang, W., Cheng, H.-M., Silva, S.R.P., 2020. Critical review of recent progress of flexible perovskite solar cells. Mater. Today 39, 66–88.
- Zhao, Y., Zhu, K., 2016. Organic–inorganic hybrid lead halide perovskites for optoelectronic and electronic applications. Chem. Soc. Rev. 45, 655–689.